Preprints (www.preprints.org) | NOT PEER-REVIEWED | Posted: 19 October 2020 doi:10.20944/preprints202010.0366.v1

Article

Operational optimization at signalized metering roundabouts using cuckoo search/local search algorithm

Hong Ki An [1]*, Yao Liu [2] and Dong Sun Kim [3],

[1] Faculty of Transportation Engineering, Huaiyin Institute of Technology, Huai'an, China; hong_ki.an@mymail.unisa.edu.au
[2] Faculty of Engineering Management, Huaiyin Institute of Technology, Huai'an, China; xiaoyao_6554@163.com
[3] Department of Urban and Realty Engineering, Daejin University, Gyeonggi, Korea; kimdns@daejin.ac.kr

* Correspondence: hong_ki.an@mymail.unisa.edu.au; Tel.: +8229652855

Abstract: A metering roundabout where traffic is controlled by traffic lights with phase times influenced by queue detector occupancy might be the solution to enhance performance when there are unbalanced traffic flows at roundabouts. There have, however, been minimal studies on how the distance of the queue detector from the stop line affects signal phase time durations and the queuing lengths. This research, therefore, seeks to develop a Cuckoo Search/Local search Algorithm using parameters such as arrival volumes, conflicting volumes, detector distance and phase time to investigate the relationship of signal setting, detector location and queuing formulations. Also, some additional statistical tests were performed for the fitness of the data. In order to conduct solid model validations, model output data was compared against the AIMSUN model. The results from the analyses demonstrated that the queue detector distance can affect phase time durations and vehicle queuing lengths on the controlling approach as well as queuing lengths on the metered approach. This study showed that, based on the study for the Old Belair Road roundabout in Adelaide, South Australia, the total queue length (controlling + metered) will be minimized when the detector is relocated at 209 meters from the roundabout stop line, giving longer phase green times and resulting in decreased intersection queuing lengths.

Keywords: Metering roundabout, Detector location, AIMSUN, Cucksoo search/Local search algorithm

1. Introduction

Roundabouts can experience congestion problems, particularly during peak hours when there are unbalanced traffic conditions [1-5]. Delays on one or two approaches can be observed because entering vehicles may be interrupted by rotating vehicles. Thus, in order to form balanced traffic flow conditions and obtain enough gaps between rotating vehicles, the signalized roundabout emerged as a popular alternative, often called a metering roundabout.

Several researchers attempted to make a definition of unbalanced traffic conditions using the origin-destination factor, which is able to enhance metering roundabout capacity [6,7]. According to past studies, the operational performance on a roundabout can be exacerbated by unbalanced traffic conditions. In such cases, an effective solution is the metering roundabout leading to a decrease in queues or delays. In addition, past studies explained that vehicle movements on a roundabout and T-junction are similar and they operate individually. Another studies [7,8], however, gave a definition with respect to unbalanced conditions with the prerequisite that ingression vehicles from one approach might affect the vehicle movements on other approaches at roundabouts. According to Akçelik [9,10], the distance of the queue detector from the give-way line should be in the range of 50

– 120 meters using the probability of the blockage parameter that is used when a road has limited queue storage. The parameter describes how downstream traffic flow affects upstream congestions.

Fortuijn [11], a study of the queue detector distance from the stop line is important because signal phase durations are greatly influenced by detector occupancy rates with respect to the metering roundabout. Fortuijn [11], also tried to find the queue detector distance (demand detector) using the Pollaczek-Khinchine M/M/1 waiting-time formula. However, this study was based on a different type of control metering roundabout which had the queue detector installed on the dominant approach and a delay detector on the sub-dominant approach.

Sergey et al. [12] analyzed the associated characteristics of traffic signal control and dynamic guidance systems, using intelligent technology and fusion technology to study its intelligent collaboration, and proposed a structural framework for urban traffic signal control and traffic guidance system intelligent collaboration, which is controlled by traffic signals. Hao et al. [13] discussed the problem of traffic demand balance under the condition of limited environmental capacity of road sections using mathematical programming methods to describe the continuous network balance problem of demand changes in the waiting situation. However, the impact of urban traffic signals on the passage capacity of road sections and environmental pollution at intersections and how to meet the increasing traffic demand by increasing the traffic demand of the entire network was not considered.

Brederode and Verlinden [14] considered how to increase network traffic demand under traffic signal control conditions. Lin et al. [15] studied the user balance distribution problem and the system optimal distribution problem based on emissions. Ding et al. [16] discussed the generalized user optimal equilibrium assignment problem and the generalized system optimal equilibrium assignment problem. However, the determination of the user balance allocation model considered the problem of continuous balance network design. Fontaine and Minner [17] combined the road environment capacity limitation, the optimal traffic signal setting problem and the urban traffic discrete network design problem. However, the construction of new road sections maximizes the traffic demand to meet the growing traffic demand in the city and the maximum demand of the transportation network can meet the requirements of modern urban environmental protection through the restriction of road environmental capacity.

At present, many researches on the optimization and control of urban traffic are mostly based on the optimization of traffic flow distribution in the urban transportation network, or the optimal control based on the shortest time between the traveler's starting points, or the largest urban capacity. Optimal control of traffic flow distribution optimizes for the signal period or signal time interval mostly using conventional optimization methods, such as the genetic algorithm, particle swarm optimization, adaptive neuro fuzzy method, etc [18-20]. Therefore, there are still relatively little research to investigate detector locations, which is an important parameter affecting the entire performance of the roundabout.

This study investigates the optimal signal operational using Cuckoo Search/Local search Algorithm. The detail of detector locations and the queuing length on major (controlling) approach and minor (metered) approach presented in detail. The proposed method simulated using Matlab software and compared with microscopic simulation model AIMSUN. To achieve this purpose, drone footage data will be used in the process of CS/LS algorithm, and AIMSUN model development, calibration and validation. The result shows that the metering roundabout can reduce the queues of the major (controlling) approach. However, the queuing length on the minor approach (metered) would be longer due to the red signal blocking vehicles from entering. Furthermore, Geoff E. Havers (GEH) tests will be performed to assess the fitness of the model in AIMSUN.

 doi:10.20944/preprints202010.0366.v1

2. Research background

2.1. The Metering Roundabouts Model

The concept of metering roundabout is described in Figure 1. In this roundabout, detectors are installed on the controlling (dominant) approach and the traffic signals on the metered (sub-dominant) approach are differently set up from traditional ones.

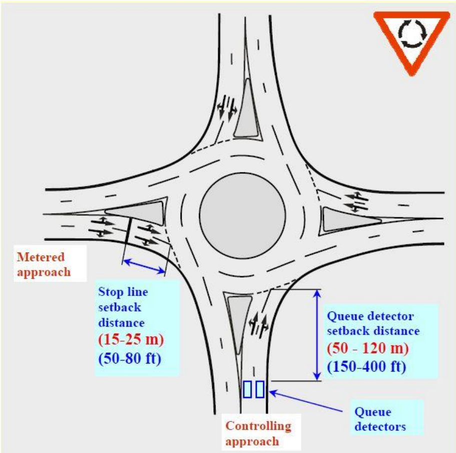

Figure 1. Concept of metering roundabout [10].

Stevens [1], Azhar and Svante [21], and Mosslemi [22] mentioned that a signal roundabout can be grouped into three categories: traffic flow control, operation time and number of approaches controlled as presented in Table 1.

Table 1. Categories of signal roundabout.

Classification	Control Type	Description
Traffic flow control	Direct control	Entering traffic flow and circulatory traffic flows are controlled by signals
	Indirect control	Only entering traffic flows are controlled by signals
Operation time	Full time control	Signal is operated for 24 hours
	Part time control	Signal is activated by time of day or by detectors
Number of approaches controlled	Full control	All approaches are controlled by signals
	Partial control	Approaches are controlled by signals while the remaining approaches operate under give way control

Among the categories of signal roundabouts given in the table above, unbalanced traffic flow conditions usually occur during peak hours, thus, indirect with part-time control is the most appropriate control system [1,3,7,9]. In addition, the simple form of a signal metering roundabout has a valuable benefit-cost ratio because it is easy to operate with low installation cost [23].

It is also the case that the metering signal phase lengths can be determined by the position of the approach detector. An et al. [24] applied the concept and formulated the queuing length models at metering roundabouts in order to estimate the queuing length based on detector locations and signal phase times. In their study numerical models were formulated with six main parameters that significantly affect the formation of queuing length for each approach. Three variables (i.e. arrival volume, conflict volume and vehicle space) commonly have a positive relationship to queuing length. However, detector location on the controlling and metered approaches, vehicle presence time on the controlling and metered approaches, and signal phase green and red time duration can be differently applied. Therefore, the queuing length estimation model in controlling and metered approaches can be expressed in Equation 1 and 2 [24].

$$Q_{con} = \frac{\left(\frac{P_{gre}}{T} \times \frac{\frac{V_i}{NL}}{T} \times \frac{\frac{VC_i}{NL}}{T} \times DL_C \times PT_C \times VS\right)}{DL_M \times PT_M} \times 6700 \quad (1)$$

$$Q_{met} = \frac{\left(\frac{P_{red}}{T} \times \frac{\frac{V_i}{NL}}{T} \times \frac{\frac{VC_i}{NL}}{T} \times DL_M \times PT_M \times VS\right)}{DL_C \times PT_C} \times 15000 \quad (2)$$

The phase green and red times can vary theoretically by up to 300 seconds (5 minutes). To explain in detail, in a cycle of 300 seconds, the green and red time may take a share of the cycle time. Thus, a relationship between Pred and Pgre is presented in Equation 3.

$$P_{red} = 300 - P_{gre} \quad (3)$$

Where Qcon is the queuing length of the controlling approach (m), Qmet is the queuing length of the metered approach (m), Pgre is the green time (s), Pred is the red time (s), NL is the number of the lane, Vi is the arrival volume of subject i approach (vehs), Vci is the conflict volume against subject i approach, DL_C is the detector location on the controlling approach (km), DL_M is the detector location on the metered approach (km), VS is the vehicle space (m), PT_C is the vehicle presence time on the Detector C (s), PT_M is the vehicle presence time on the Detector M (s), and T is time.

The Old Belair Road roundabout has no detector on the metered approach, thus, constant "1" was applied for the cases (i.e. DLM = 1 and PTM = 1).

2.2. The Cuckoo Algorithm

The Cuckoo Search (CS) algorithm is an emerging algorithm that combines the common cuckoo breeding mechanism with the local search (LS) method [25,26,27]. The CS algorithm has a good initial search ability, but poor optimization ability in the later periods, low search accuracy and slow convergence speed, so it needs to be improved for multi-objective optimization.

For a 1-dimensional optimization problem, d variables are needed:

$$x = [x_1, x_2, \ldots\ldots, x_d] \quad (4)$$

The Levy Flight location update formula is：

$$x_i^{t+1} = x_i^t + \alpha \oplus L(\lambda) \qquad i = (1,2, \ldots n) \quad (5)$$

$$L(\lambda) \sim u = t^{-\lambda}, \qquad 1 < \lambda \le 3 \quad (6)$$

Where: x_i^{t+1} is the updated bird's nest position; x_i^t t is the current bird's nest position; $\oplus$ is the point-to-point multiplication; α is the step size; $L(\lambda)$ is the search path; u is the standard normal variable and u follows the normal distribution of $N(0, \sigma_u^2)$.

If the parasitic nest's communication threshold is δ, the current optimal parasitic nest position is x_b^t and the probability of parasitic nest i to communicate is p_i. If $p_i < \delta$, then the communication in Equation 7 is performed.

$$x_i^t = r \cdot x_i^t + (1-r) \cdot x_b^t, \qquad i = 1,2, \ldots, n \quad (7)$$

In the formula: x_i^t is the bird's nest position after communication; *r* is a random number between (0,1). When the CS algorithm parameters are set, it is found that the probability p_a and the step size α are fixed, which will cause the algorithm's convergence and search speed to deteriorate. When setting the two, if $p_a$is small and α is large, it will increase the number of iterations. If $p_a$is large and α is small, it will improve the convergence speed, but the optimization ability is poor. Therefore, setting the two as dynamic quantities causes change with the number of iterations, which can both improve the convergence speed of the algorithm and increase its search accuracy. The specific improvement formula is as follows:

$$p_a(t) = p_{a,max} - \frac{t}{g}(p_{a,max} - p_{a,min}) \tag{8}$$

$$\alpha(t) = \alpha_{max}\exp\,(c.t) \tag{9}$$

$$c = \frac{1}{g}\ln\left(\frac{\alpha_{min}}{\alpha_{max}}\right) \tag{10}$$

Where: $p_a(t)$ is the probability function of discovery; $\alpha(t)$ is the step function; c is the intermediate variable; $p_{a,max}, p_{a,min}$ are the control parameters of p_a; g is the number of iterations ; *t* is the current evolution algebra; $\alpha_{max}, \alpha_{min}$ are the control parameters of the step size, respectively.

For the minimization of multi-objective problems, if the solution vector, $\boldsymbol{x_1}$, $\boldsymbol{x_2}$satisfy Equation 11, then $\boldsymbol{x_1}$ dominates $\boldsymbol{x_2}$:

$$\forall_i \in \{1,2,\ldots.,M\}: f_i(x_1) \le f_i(x_2) \tag{11}$$

$$\exists_i \in \{1,2,\ldots.,M\}: f_i(x_1) \le f_i(x_2) \tag{12}$$

Where *M* is the number of solution vectors; $f_i(x_1), f_j(x_1)$ are the minimum objective function values; $f_i(x_2), f_j(x_2)$ are the maximum objective function values.

After the optimal solution is generated, the optimal satisfactory solution is calculated using the CS algorithm which provides the optimal detector location and signal solution for the roundabout. The satisfaction of the objective function is in Equation 13.

$$\mu_i = \begin{cases} 1 & f_i \le f_{i,min} \\ \dfrac{f_{i,max} - f_i}{f_{i,max} - f_{i,min}} & f_{i,min} < f_i < f_{i,max} \\ 0 & f_i \ge f_{i,max} \end{cases} \tag{13}$$

Where μ^krepresents the satisfaction of the *i*-th optimal solution; f_i is the *i*-th objective function value; $f_{i,min}$, $f_{i,max}$ are the minimum and maximum objective function values, respectively.

2.3. The Local Search

In order to improve the solution quality, a LS scheme was carried out, in which it explored the area less congested in the current archive which may obtain more non-dominated solutions [28,29]. The general operation of the scheme is described in the following steps.

Step 1: It began with a randomly selected point ($x_m \in R_n$) $\in E^t$, and the set step lengths Δx_i in all of the organized directions u_i, $i = 1,\ldots,n$. Setting $m = 0$, and that m was the size of E^t.

Step 2: Setting the beginning of the counter $m = m + 1$, and $h = 1$ where h is the number of trials ($h = 1,\ldots,h_{max}$) to obtain a more preferred solution than x_m .

Step 3: The variable x_i was perturbed around the present temporary base point x_m to get the new provisional base point x'_m as:

Preprints (www.preprints.org) | NOT PEER-REVIEWED | Posted: 19 October 2020 doi:10.20944/preprints202010.0366.v1

$$x'_m = \begin{cases} x_m - \Delta x_i\, u_i & if\ \ f^-(*) > (f(*) \cap f^+(*)) \\ x_m & if\ \ f(*) > (f^-(*) \cap f^+(*)) \\ x_m + \Delta x_i u_i & Else\ \ if\ \ f^+(*) > f(*) \end{cases} \tag{14}$$

$$\forall_0 i = 1, 2, \ldots\ldots, n$$

Where, $f(*) = f(X_m)$, $f^+(*) = f(X_m + \Delta x_i u_i)$, $and\ f^-(*) = f(X_m - \Delta x_i u_i)$. Besides, $f(*)$ was assumed as the valuation of the objective functions at a point.

Step 4: The condition of point X_m was unchanged.

Although the number of trials h was not satisfied, the step length Δxi was decreased by using the next dynamic equation,

$$\Delta x_i = \Delta x_i (1 - (r)^{h/h_{max}} \tag{15}$$

Where, r is a random number, and $r \in [0, 1]$, then, step 3 was repeated.

Step 5: Or else, if x'_m was preferred than, x_m,$(i.e., f(x'_m) > f(x_m)$ then, the new base point would be x'_m, hence, step 6 must be repeated.

Step 6: Also, it can be aided by the base points x_m and x'_m , in establishing a pattern direction S, as follows:

$$S = x'_m - x_m \tag{16}$$

Point x''_m had to be identified.

$$x''_m = x'_m + \lambda S \tag{17}$$

Where, λ is the step length, which could be taken as $\lambda = 1$.

Step 7: If $f\ (x''_m) \leq f(x'_m)$ set $x_m = x'_m$, then step 4 had to be repeated.

Step 8: Or else, if $f(x''_m) > f(x'_m)$, set $x_m = x'_m$, $x'_m = x''_m$, then, step 6 had to be repeated.

Step 9: If the x_m had been the best possible points, they must be compared with predefined parameters to get to the end.

3. Data collection

Data collection for one hour during peak period was carried out at Old Belair Road roundabout in Adelaide, Australia for three days as below:

- 1st survey: October 7, 2015 between 07:45 and 08:45 (Wednesday)
- 2nd survey: October 8, 2015 between 07:25 and 08:25 (Thursday)
- 3rd survey: November 17, 2015 between 07:50 and 08:50 (Tuesday)

There are six major parameters for calculating queuing length on each approach, and data were collected from three sources: field survey using drones, Sydney Coordinated Adaptive Traffic System (SCATS) and DPTI documents, as presented in Table 2.

For traffic volumes and signal phase time data, SCATS data were used. The SCATS, developed in Australia, is now used internationally as an adaptive traffic signal control [30]. SCATS obtains traffic information from detectors located behind the stop line on each lane. Traffic data information from SCATS includes two types, traffic count data and traffic signal operation data. All these counts are detector based, further, this data is stored in a NEXUS database managed by DPTI at the Barbara Hardy Institute, University of South Australia, and the use of historical data is also available [31]. SCATS VS data can be extracted from a selected period of a minimum of five minutes using Traffic Reporter.

Table 2. Collected data.

October 7th								
	North(metered) approach			South(controlling) approach			Phase time	
Time	V_{CN}	V_N	Queue	V_{CS}	V_S	Queue	Pgre	Pred
07:45-07:50	5 veh	52 veh	600 m	42 veh	69 veh	80 m	258 s	42 s

07:50-07:55	4 veh	50 veh	800 m	48 veh	49 veh	60 m	243 s	57 s
07:55-08:00	5 veh	67 veh	500 m	44 veh	83 veh	150 m	170 s	130 s
08:00-08:05	8 veh	57 veh	910 m	48 veh	80 veh	130 m	150 s	150 s
08:05-08:10	7 veh	60 veh	620 m	37 veh	74 veh	135 m	150 s	150 s
08:10-08:15	4 veh	44 veh	400 m	42 veh	72 veh	155 m	182 s	118 s
08:15-08:20	7 veh	53 veh	665 m	41 veh	63 veh	150 m	175 s	125 s
08:20-08:25	5 veh	65 veh	490 m	50 veh	86 veh	125 m	160 s	140 s
08:25-08:30	6 veh	64 veh	535 m	44 veh	67 veh	135 m	160 s	140 s
08:30-08:35	5 veh	57 veh	440 m	44 veh	57 veh	70 m	160 s	140 s
08:35-08:40	6 veh	57 veh	420 m	53 veh	45 veh	50 m	160 s	140 s
08:40-08:45	6 veh	71 veh	220 m	39 veh	55 veh	50 m	160 s	140 s
October 8th								
07:10-07:15	6 veh	37 veh	620 m	29 veh	77 veh	65 m	218 s	83 s
07:15-07:20	5 veh	43 veh	650 m	35 veh	88 veh	70 m	218 s	83 s
07:20-07:25	6 veh	40 veh	650 m	31 veh	91 veh	150 m	206 s	94 s
07:25-07:30	6 veh	57 veh	720 m	44 veh	94 veh	160 m	195 s	105 s
07:30-07:35	7 veh	35 veh	580 m	28 veh	109 veh	160 m	121 s	179 s
07:35-07:40	6 veh	58 veh	950 m	43 veh	118 veh	175 m	115 s	185 s
07:40-07:45	7 veh	60 veh	920 m	48 veh	127 veh	180 m	99 s	201 s
07:45-07:50	5 veh	48 veh	830 m	38 veh	116 veh	180 m	80 s	220 s
07:50-07:55	6 veh	54 veh	860 m	46 veh	112 veh	185 m	61 s	239 s
07:55-08:00	5 veh	62 veh	910 m	52 veh	102 veh	165 m	52 s	248 s
08:00-08:05	5 veh	65 veh	1000 m	52 veh	88 veh	115 m	56 s	244 s
08:05-08:10	6 veh	56 veh	1100 m	42 veh	103 veh	160 m	58 s	242 s
November 17th								
07:50-07:55	7 veh	64 veh	680 m	49 veh	74 veh	70 m	155 s	145 s
07:55-08:00	7 veh	75 veh	768 m	59 veh	73 veh	70 m	165 s	135 s
08:00-08:05	8 veh	53 veh	700 m	42 veh	90 veh	50 m	152 s	148 s
08:05-08:10	9 veh	52 veh	905 m	40 veh	97 veh	70 m	128 s	172 s
08:10-08:15	7 veh	51 veh	790 m	40 veh	95 veh	60 m	110 s	190 s
08:15-08:20	8 veh	63 veh	1000 m	55 veh	73 veh	150 m	125 s	175 s
08:20-08:25	7 veh	70 veh	835 m	52 veh	78 veh	170 m	148 s	152 s
08:25-08:30	5 veh	76 veh	505 m	55 veh	49 veh	130 m	170 s	130 s
08:30-08:35	7 veh	71 veh	650 m	48 veh	64 veh	135 m	193 s	107 s
08:35-08:40	5 veh	63 veh	60 m	41 veh	79 veh	160 m	215 s	85 s
08:40-08:45	4 veh	59 veh	45 m	36 veh	66 veh	130 m	237 s	63 s
08:45-08:50	6 veh	43 veh	95 m	32 veh	66 veh	45 m	250 s	50 s

4. Proposed methods

In a metering roundabouts system model, the typical transfer function can be considered as shown in figure 2. The optimal detector location and traffic signal of the roundabout model is based on ensuring the minimum queuing length load, while satisfying the dual-objective with minimum queues on controlling and metered approaches. In the roundabout model, the constraint conditions of the objective function are as follows.

(1) The controlling approach objective:

$$min f_1 = Q_{Con}(x_1, x_2) \tag{18}$$

Where Q_{Con} is controlling approach in Equation 1; x_1, x_2 are the DLc detector location and $Pgre$ green time; f_1 is the objective function of controlling queuing length.

(2) The metering approach objective:

$$min f_2 = Q_{met}(x_1, x_2) \tag{19}$$

Preprints (www.preprints.org) | NOT PEER-REVIEWED | Posted: 19 October 2020 doi:10.20944/preprints202010.0366.v1

Where Q_{met} is metering approach in Equation 2; f_2 is the objective function of metering queuing length.

(3) The total queuing goals:

Integrating the two objective functions, the objective function used to identify the function of metering roundabouts system can be calculated as:

$$minY(x) = min[f_1(P_1), f_2(P_2)] \quad (20)$$

$Y(x)$ is the objective function after integration.

The optimization process is to extract the optimal parameters Pgre, Pred, NL, Vi, Vci , Vs, and DLc, which makes for minimum queue (see Table 2).

Where, the searching area of the coefficients is set according to the experience, Pgre=160~258 seconds, Pred=43~150 seconds, VN=35~71 vehs, VS=45~116 vehs, VcN=4~9 vehs, VCS=28~59 vehs, Vs=7 meters, DLc=50~250 meters, PTc=4 Seconds, and PTm=3 Seconds, NLcon=2 lanes, NLmet=1 lane.

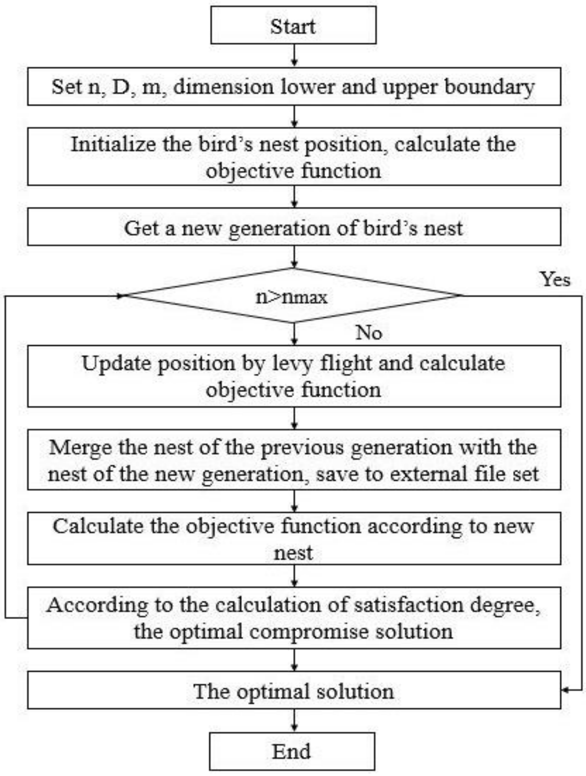

Figure 2. Block diagram of optimize queuing length.

5. Result and discussion

This section presents model verification using AIMSUN7 software to compare the optimum detector locations between cuckoo search/local search algorithm and AIMSUN results. In order for metering roundabout modelling, three procedures including modelling, calibration and validation were implemented. Moreover, in order to fit AIMSUN model output to the field data, the GEH statistical test was performed. The GEH statistic, as shown in Equation 21, is a type of chi-squared statistic and used for goodness-of-fit in transport engineering [32,33,34]. If the GEH value is less than five, the model results fit with the observed data well [34,36].

$$GEH = \sqrt{\frac{(V-E)^2}{(E+V)^{/2}}} \quad (21)$$

Where, E is the estimated output by model, and V is the observation.

5.1. Modelling of Old Belair Road Metering Roundabout

For the layout modelling, the Old Belair Road roundabout was extracted using the function “template create” in AIMSUN 7 as presented in Figure 3. The current detector was installed on the southern approach at a distance of 115 meters with a traffic signal used on the northern approach for the peak periods.

Queuing lengths on each approach were collected using drones in five-minute intervals in this study and traffic volumes in Table 2 on each approach (Northern approach: VN, Southern approach: VS, Western approach: VW, and Eastern approach: VE) was input for performance evaluation. In order for more precise analysis, 20 minutes of warm-up and cool-off periods were applied before and after the one-hour modelling durations.

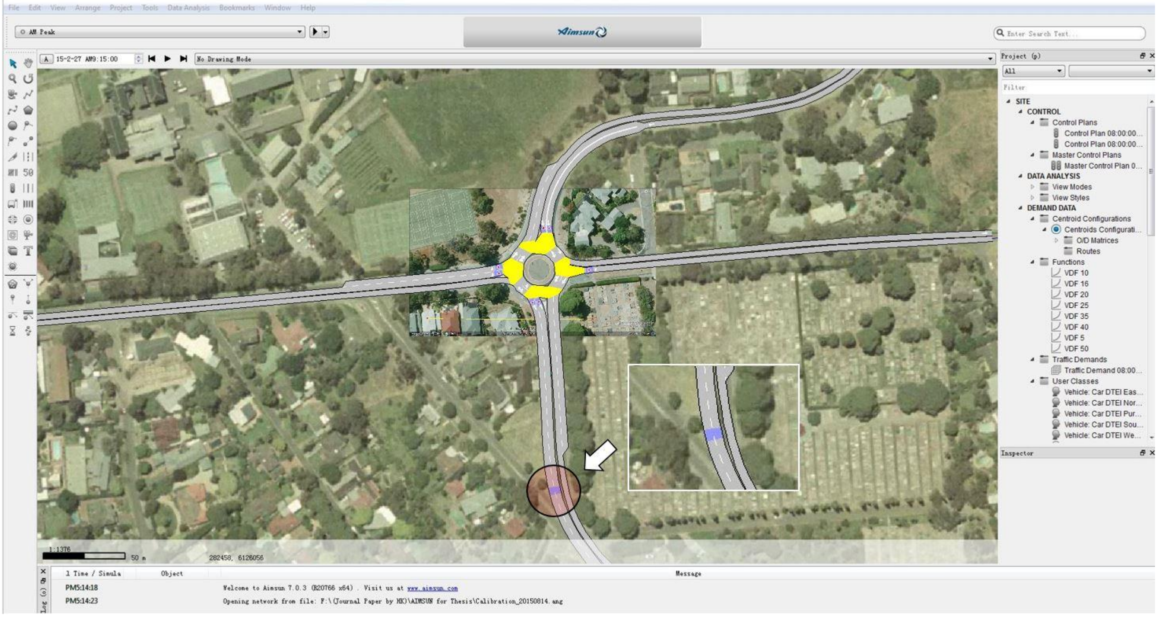

Figure 3. Old Belair Road metering roundabout in AIMSUN 7.

The metering system was set with control strategies under the “traffic management” function in AIMSUN 7, which creates a connection between the installed traffic light and detectors for operating the metering system according to queuing length on the controlling (northern) approach. Start and stop triggers were specified for monitoring the occupancy time in the queue detector zone, as shown in Figure 4.

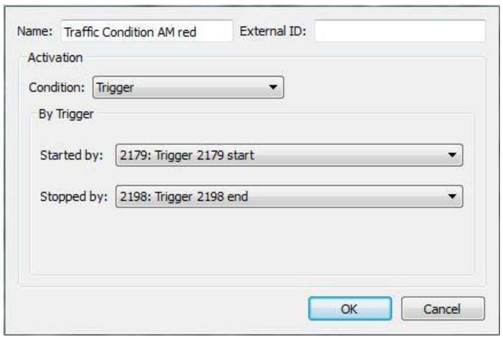

Figure 4. Trigger setting for detector operation.

In addition, the occupancy value can be defined as the “percentage of cycle time that the detector detected presence in the last cycle”, as shown in Equation 22.

$$Occupancy = \frac{\sum_{i=1}^{Total\ number\ of\ intervals} t_{final}(i, cycle) - t_{init}(i, cycle)}{Cycle} \times 100 \quad (22)$$

Where, $t_{init}(i, cycle)$ is an initial time, $t_{final}(i, cycle)$ is a final time, and Cycle is 120 seconds.

This study input 55 occupancy value as starting detection and a value of 20 was specified for detection end.

In order to duplicate the real-life signal phase timing and double cycle, two control plans were applied as follows:

- Control Plan 1: Queuing length is shorter than detector location
- Control Plan 2: Queuing length is longer than detector location

Control Plan 1 is for normal conditions which is that vehicle queues did not reach the detector on the controlling approach. In this case, maximum green time (90 seconds: 45 + 45 seconds) and minimum green time (42 seconds: 21 + 21 seconds) were input (see Table 2). Control Plan 2 is used during metering system activation and if the detector detects the queues on the controlling approach for three seconds, AIMSUN 7 will switch to Control plan 2. When the detector occupancy is cleared, Control plan 1 would be activated automatically.

5.2. Model Calibration and Validation

After modelling, parameter calibration is necessary for matching the queuing length from the drone data. This study compared two days queuing length data for the model calibration on October 7th and 8th, and November 17th data was compared for the model validation. Maximum speed (approaching approach and exiting approach), visibility distance, yellow-box speed, maximum desired speed (vehicle) were adjusted as shown in Table 3.

Table 3. Calibrated parameters.

Parameters	Default value	Adjusted value
Maximum speed (approaching)	60km/h	50km/h
Maximum speed (exiting)	60km/h	36km/h
Visibility distance	10m	6m(north), 12m(south)
Yellow-box speed	10 km/h	4km/h(north), 5km/h(south)
Maximum desired vehicle speed	120km/h	60km/h

With the adjusted values in AIMSUN, the queuing lengths on the controlling and metered approaches were compared in Table 4. It can show that the queuing length of AIMSUN outputs are closely matched to the field data on the north and south approaches during the peak hour.

Table 4. The queuing length comparison between drone data and AIMSUN.

Time	Oct 7th				Time	Oct 8th			
	North		South			North		South	
	D(m)	A(m)	D(m)	A(m)		D(m)	A(m)	D(m)	A(m)
07:45-07:50	600	520	80	70	07:10-07:15	550	540	70	75
07:50-07:55	800	740	60	70	07:15-07:20	600	620	60	70
07:55-08:00	500	530	150	125	07:20-07:25	700	760	90	100
08:00-08:05	910	950	130	140	07:25-07:30	850	820	140	150
08:05-08:10	620	630	135	140	07:30-07:35	920	960	150	135
08:10-08:15	400	450	155	150	07:35-07:40	690	730	160	150
08:15-08:20	665	700	150	160	07:40-07:45	700	710	155	160
08:20-08:25	490	510	125	130	07:45-07:50	550	520	140	160
08:25-08:30	535	565	135	130	07:50-07:55	600	620	150	170
08:30-08:35	440	395	70	80	07:55-08:00	520	535	150	145
08:35-08:40	420	390	50	70	08:00-08:05	380	390	80	95
08:40-08:45	220	250	50	70	08:05-08:10	270	250	60	65

* D = Drone data, A = AIMSUN output

In addition, the GEH test was conducted for model calibration between the drone survey and AIMSUN output. Two days' data (October 7th and 8th) were used as presented in Table 5 and the GEH values were less than five in all periods. Thus, it can be seen that AIMSUN results fit with drone data well and model calibration was successfully conducted.

Table 5. GEH results for model calibration.

	Oct 7th			Oct 8th		
Statistic	**Time**	**North**	**South**	**Time**	**North**	**South**
GEH	07:45-07:50	3.38	1.15	07:10-07:15	0.42	0.59
	07:50-07:55	2.16	1.24	07:15-07:20	0.80	1.24
	07:55-08:00	1.32	2.13	07:20-07:25	2.22	1.03
	08:00-08:05	1.31	0.86	07:25-07:30	1.03	0.83
	08:05-08:10	0.40	0.42	07:30-07:35	1.30	1.25
	08:10-08:15	2.42	0.40	07:35-07:40	1.50	0.80
	08:15-08:20	1.33	0.80	07:40-07:45	0.37	0.40
	08:20-08:25	0.89	0.44	07:45-07:50	1.29	1.63
	08:25-08:30	1.27	0.43	07:50-07:55	0.81	1.58
	08:30-08:35	2.20	1.15	07:55-08:00	0.65	0.41
	08:35-08:40	1.49	2.58	08:00-08:05	0.50	1.60
	08:40-08:45	1.95	2.58	08:05-08:10	1.24	0.63
Average GEH	07:45-08:45	1.67	1.18	07:10-08:10	1.02	1.00

For model validation, November 17th data was used. Table 6 shows the queuing length of drone and AIMSUN on the north and south approaches in five-minute periods, and the GEH values. Similar to model calibration, the queuing length on the north and south approaches match well and the GEH values are all less than five. Thus, it can be seen that the AIMSUN outputs are reliable.

Table 6. GEH results of model validation.

	Nov 17th						
Time	**North**		**South**		**Statistic**	**North**	**South**
	D(m)	**A(m)**	**D(m)**	**A(m)**			
07:50-07:55	680	640	65	70	GEH	1.55	0.61
07:55-08:00	770	750	65	80		0.72	1.76
08:00-08:05	700	650	55	70		1.92	1.90
08:05-08:10	905	880	65	60		0.84	0.63
08:10-08:15	790	800	60	70		0.35	1.24
08:15-08:20	1005	910	155	160		3.07	0.39
08:20-08:25	835	725	170	180		3.94	0.75
08:25-08:30	505	585	130	145		3.43	1.28
08:30-08:35	650	550	135	160		4.08	2.05
08:35-08:40	60	85	160	170		2.93	0.78
08:40-08:45	45	70	130	110		3.30	1.83
08:45-08:50	95	110	45	60		1.48	2.07
					Average GEH	2.30	1.27

5.3. Optimal Detector Location in AIMSUN

In order to find the optimum detector location on November 17th, the detector on the controlling approach was moved in 25-meter increments between 50 meters and 225 meters in AIMSUN. Then, the total queuing length (north + south) from 10 replications for peak hour is presented in Table 7.

Table 7. Queuing length on the north and south in accordance with detector moves.

Time	DL = 50m		DL =75m		DL=100m		DL=125m	
	N(m)	S(m)	N(m)	S(m)	N(m)	S(m)	N(m)	S(m)
07:50-07:55	1,320	25	820	45	795	60	720	95
07:55-08:00	1,300	30	900	50	850	75	700	115
08:00-08:05	1,250	30	920	50	860	70	820	120
08:05-08:10	1,630	40	920	40	830	80	770	110
08:10-08:15	2,465	40	1,330	50	910	100	810	135
08:15-08:20	2,745	45	1,680	70	1,255	125	860	165
08:20-08:25	2,550	30	1,740	80	920	145	700	190
08:25-08:30	2,010	40	1,305	50	780	120	570	150
08:30-08:35	1,860	40	1,425	60	750	130	555	170
08:35-08:40	960	30	485	75	180	135	80	175
08:40-08:45	925	30	425	70	140	100	75	125
08:45-08:50	900	35	325	50	115	100	75	130
Average (N+S)	1,694		1,080		802		701	
Time	**DL=150m**		**DL=175m**		***DL=200m***		**DL=225m**	
	N(m)	**S(m)**	**N(m)**	**S(m)**	**N(m)**	**S(m)**	**N(m)**	**S(m)**
07:50-07:55	560	105	430	110	290	135	330	165
07:55-08:00	580	105	450	125	340	150	380	170
08:00-08:05	650	110	490	140	460	160	450	190
08:05-08:10	680	135	510	165	470	185	460	190
08:10-08:15	700	150	520	180	430	210	500	220
08:15-08:20	825	190	555	200	480	240	520	255
08:20-08:25	655	195	660	215	560	225	550	250
08:25-08:30	520	160	530	185	520	205	500	235
08:30-08:35	525	160	550	180	520	185	510	220
08:35-08:40	80	170	80	200	40	230	40	240
08:40-08:45	80	130	75	150	45	170	45	200
08:45-08:50	65	130	70	135	45	155	40	195
Average (N+S)	638		575		***538***		571	

The optimum detector location reflects the minimum queuing length considering both (controlling and metered) approaches. When the detector location is at 50 meters, queuing length of two approaches was on average 1,694 meters for one hour. Thus, the detector location of 50 meters is the worst distance. When the detector location is at 200 meters, the sum of both approaches was on average 538 meters. In this case, queuing length can be decreased by around 1150 meters for peak hour.

5.4. Best Detector Location in Cuckoo Search/Local Search Algorithm

In order to verify the proposed optimization algorithm to determine the detector location in accordance with arrival volume and conflicting volume, the two signal timing schemes are obtained

Preprints (www.preprints.org) | NOT PEER-REVIEWED | Posted: 19 October 2020 doi:10.20944/preprints202010.0366.v1

by using Equation 3, which are respectively recorded as optimize Equation 1 and 2. Furthermore, the tuning parameters for the CS/LS proposed algorithm, Levy exponent (β)=0.25, number of iterations=50, number of nests=10 were set in order to get accurate results.

Table 8 shows that each iteration indicates different queuing lengths on the controlling and metered approach in accordance with a relationship between detector locations and phase green time. Total queuing length (controlling + metered approaches) looks steady after 40th iteration, which means 210 meters of detector location is the best detector location.

Table 8. Effect of detector location and signal time.

No. Iteration	Pgre (s)	DLC (m)	Qcon (m)	Qmet (m)	Qtotal (m)	No. Iteration	Pgre (s)	DLC (m)	Qcon (m)	Qmet (m)	Qtotal (m)
1	180.8	57.5	46.3	1206.6	1253.0	26	190.6	196.6	166.4	324.9	491.3
2	203.6	55.8	50.6	1005.5	1056.2	27	210.9	147.7	138.6	351.5	490.1
3	178.4	73.4	58.3	964.2	1022.5	28	222.2	123.4	122.2	366.7	488.9
4	161.5	86.9	62.5	927.3	989.8	29	176.9	245.9	193.7	291.5	485.2
5	182.8	77.3	62.9	883.2	946.1	30	252.9	67.1	75.6	408.5	484.0
6	179.5	102.3	81.8	685.7	767.5	31	190.1	227.0	192.1	281.9	474.0
7	189.6	102.4	86.5	627.5	714.0	32	211.1	165.7	155.7	312.5	468.2
8	183.5	112.2	91.7	604.7	696.4	33	203.6	194.2	176.0	289.1	465.2
9	182.6	117.0	95.2	584.1	679.2	34	195.3	234.6	204.0	259.8	463.8
10	196.8	109.3	95.8	549.5	645.3	35	237.6	102.5	108.4	354.7	463.1
11	168.1	151.5	113.4	506.8	620.2	36	214.7	168.9	161.5	294.0	455.5
12	213.3	96.3	91.4	524.4	615.8	37	224.9	137.7	137.9	317.4	455.4
13	233.2	72.2	75.0	538.9	613.9	38	241.8	97.4	104.9	348.0	452.9
14	195.1	147.7	128.3	413.5	541.9	39	204.7	235.7	214.8	235.5	450.3
15	244.4	69.7	75.9	464.1	539.9	40	***208.7***	***210.2***	***195.3***	***253.0***	***448.3***
16	205.1	131.7	120.3	419.6	539.8	41	***208.7***	***210.2***	***195.3***	***253.0***	***448.3***
17	228.7	94.3	96.0	440.3	536.3	42	***208.7***	***210.2***	***195.3***	***253.0***	***448.3***
18	224.8	101.6	101.7	431.2	532.8	43	***208.7***	***210.2***	***195.3***	***253.0***	***448.3***
19	177.1	185.9	146.6	385.0	531.6	44	***208.7***	***210.2***	***195.3***	***253.0***	***448.3***
20	178.9	192.2	153.1	366.9	520.0	45	***208.7***	***210.2***	***195.3***	***253.0***	***448.3***
21	197.9	159.3	140.4	373.3	513.6	46	***208.7***	***210.2***	***195.3***	***253.0***	***448.3***
22	164.3	230.9	168.9	342.2	511.1	47	***208.7***	***210.2***	***195.3***	***253.0***	***448.3***
23	222.6	113.7	112.7	396.5	509.2	48	***208.7***	***210.2***	***195.3***	***253.0***	***448.3***
24	215.0	129.1	123.6	383.4	507.0	49	***208.7***	***210.2***	***195.3***	***253.0***	***448.3***
25	183.0	209.2	170.5	325.5	496.0	50	***208.7***	***210.2***	***195.3***	***253.0***	***448.3***

Figure 5 shows the total queuing length for optimization arrived at for different detector locations and signal times. Optimizations from Equations 1 and 2 are calculated based on collected traffic flow. From the 1st to 13th iteration, the queuing length on metered approach is decreased dramatically by 55.3 percent (from 1,206 meters to 539 meters). The queuing length on the controlling approach, however, is slightly increased by 30 meters. Thus, the total queuing (controlling + metered) length is 613.9 meters for one hour (51 percent decrease). On the other hand, there is not much difference between the 14th and 40th iterations and the gap in the total queuing length is only 93.6

Preprints (www.preprints.org) | NOT PEER-REVIEWED | Posted: 19 October 2020 doi:10.20944/preprints202010.0366.v1

meters an hour. It can be seen that as the iteration is repeated, the queuing length on the controlling approach is increased while the queuing length on the metered approach is decreased. The total queuing length cannot be changed after the 40th iteration by CS/LS algorithm, which means detector location at 210 meters is the optimal queuing length on the controlling and metered approaches.

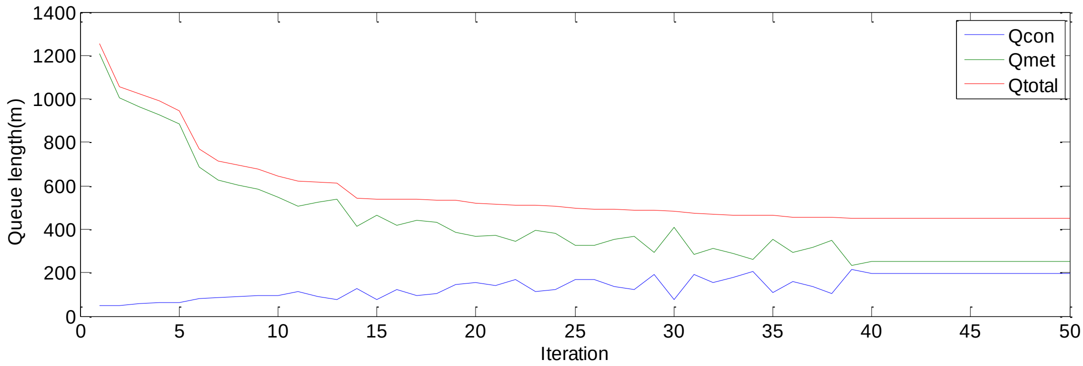

Figure 5. Optimizing the location and Green time signal of Total queuing length.

Figure 6 illustrates a relationship between detector location and signal green time with iteration increases in CS/LS algorithm (left-side y axis is detector location and right-side y axis is signal green time). Each iteration finds the best phase green time to minimize the queuing length on the controlling and metered approaches. The 30th iteration indicates that the maximum green time, detector location and total queuing length are 252 seconds, 67 meters and 484 meters respectively. In addition, 208 seconds of phase green time, 210 meters of detector location indicate the optimal roundabout operation.

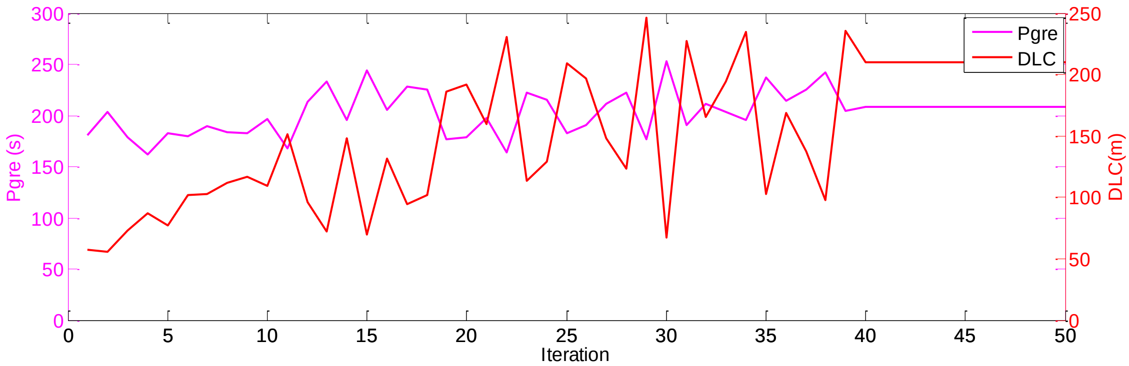

Figure 6. Relationship between detector location and signal green time.

5.5. Comparisons

The optimum detector under a variety of traffic conditions at a metering roundabout is calculated and simulated by CS/LS algorithm and AIMSUN software based on November 17th data. Table 9 shows that the result of the proposed algorithm obtained by adopting the best detector location makes the average queuing length decrease by 6.8% compared to AIMSUN. The best detector location attained from the CS/LS algorithm is 209 meters and the total queueing length is 499 meters, whereas, AIMSUN simulates that 200 meters of detector location can minimize the total queuing length by 538 meters. In addition, phase green time, average queuing length on the controlling approach, average queuing length on the metered approach match 90.3 percent, 91.7 percent and 96.1 percent respectively between the two models.

Table 9. Comparison of proposed method.

	AIMSUN software	CS/LS Algorithm	Ratio
Pgre	217s	247s	87.8%
DLc	200m	209m	95.7%
Qcon	187m	175m	91.7%
Qmet	350m	324m	96.1%
Qtotal	538m	499m	93.2%

The research result indicates that there is not much difference in detector location between CS/LS algorithm and AIMSUN software. Although the total queuing length of the two models is similar (7 percent), phase green time and queuing length on each approach is slightly different (12 percent).

6. Conclusion

This paper attempts to investigate the optimal detector location at the Old Belair Road metering roundabout using CS/LS algorithm in order to minimize the queuing length not only on the controlling, but also on the metered approaches. The outputs were compared with the microscopic simulation model AIMSUN as algorithm verification. The CS/LS algorithm indicated that detector location at 209 meters optimizes the queuing length on the controlling approach (204 meters) and metered approach (364 meters). Moreover, 247 seconds of average phase green time was calculated for the one-hour morning peak. It is quite similar to the AIMSUN model output and the differences are just nine meters in detector location and 30 seconds in phase green time. Thus, it can be expected that the CS/LS algorithm model used in this paper would save time for determining the best detector location at metering roundabouts. Furthermore, the proposed model would serve as a platform for studying the relationship between detector locations and signal phase time at metering roundabouts. Some limitations in the research are recognized, however, and could be enhanced by more comprehensive research. First, a short lane was considered as one lane and the constant "1" was applied to the queuing models, but a specific constant needs to be defined in accordance with the length of the short lane. Second, in order for a more accurate model output, more varied conditions need to be considered such, as different geometry and traffic volume.

Author Contributions: Hong Ki An arranged the whole paper writing: including conceptualization, data collection, aimsun analysis, writing original draft preparation; Liu Yao analyzed data in CL/LS algorithm; Dong Sun Kim contributed valuable ideas of improving the research and writing-review and editing.

Funding: This research received no external funding.

Acknowledgments: The authors would like to thank Dr. Ahmed N Abdalla for his great advice on CS/LS algorithm development in this study, and University of South Australia for providing aimsun software for network analysis.

Conflicts of Interest: The authors declare no conflict of interest.

References

1. Stevens, CR. Signals and Meters at Roundabouts. Paper presented at the 2005 Mid-Continent Transportation Research Symposium, Ames, Iowa, 2005.

2. Akçelik, R. Roundabout metering signals: capacity, performance and timing. *Procedia-Social and Behavioral Sciences.* **2011**, 16, 686-696.

3. Hummer, JE.; Milazzo, I.; Joseph, S.; Schroeder, B.; Salamadi, K. The Potential for Metering to Help Roundabouts Manage Peak Period Demands in the US. Transportation Research Board 93rd Annual Meeting, Washington D.C, USA, 2014.

4. An, H.K.; Yue, W.L.; Stazic B. Dual Signals Roundabout Evaluation in Adelaide using SIDRA and AIMSUN Modelling software, *Road and Transport Research.* **2017**, Volume 26, pp. 36-49.

5. Krivda, V.; Petru, J.; Macha, D.; Plocova, K.; Fibich, D. An Analysis of Traffic Conflicts as a Tool for Sustainable Road Transport. *Sustainability* **2020**, 12, 7198

6. Hagring, O. Effects of OD flows on roundabout entry capacity. In Proceedings of the 4th International Symposium on Highway Capacity, Maui, Hawaii, USA, 2000.

7. Krogscheepers, J.; Roebuck, C. Unbalanced traffic volumes at roundabouts. In Proceedings of the 4th International Symposium on Highway Capacity, Transportation Research Circular E-C018, Maui, Hawaii, 2000, 446-458.

8. Akçelik, R.; Chung, E.; Besley, M. Performance of roundabouts under heavy demand conditions. *Road and Transport Research*, **1996**, 5: 36-57.

9. Akçelik, R. Roundabouts with unbalanced flow patterns. ITE 2004 Annual Meeting, Hawaii. *USA*, 2004.

10. Akçelik, R. Capacity and performance analysis of roundabout metering signals. *TRB National Roundabout Conference, Vail, Colorado, USA*, 2005, 22-25.

11. Fortuijn, L. Robustness of roundabout metering systems (RMS). In Proceedings of the 4th international roundabout conference, *Transportation Research Board*, 16-18 April 2014, Seattle, USA.

12. Lyapin, S.; Rizaeva, Y.; Kadasev, D.; Sysoe, A. Methods to Analyze Traffic Demand Formation in Intelligent Transportation and Logistic Regional Network. *Transportation Research Procedia*, *2020*, 45, 522-529.

13. Yua, H.; Ma, R.; Zhang, H.M. Optimal traffic signal control under dynamic user equilibrium and link constraints in a general network. *Transportation Research Part B: Methodological*, **2018**, 110, 302-325.

14. Brederode, L.; Verlinden, K. Travel demand matrix estimation methods integrating the full richness of observed traffic flow data from congested networks. *Transportation Research Procedia*, **2019**, 42, 19-31.

15. Lin, S.; Pan, T.L.; Lam, W.H.K.; Zhong, R.X.; Schutter, B.D. Stochastic Link Flow Model for Signalized Traffic Networks with Uncertainty in Demand. *IFAC-Papers OnLine*, 2018, 51, 458-463.

16. Ding, Z.J.; Dai, Z.; Chen, X.M.; Jiang R. Simulating on-demand ride services in a Manhattan-like urban network considering traffic dynamics. *Physica A: Statistical Mechanics and its Applications*, **2020**, 545, 123621.

17. Fontaine, P.; Minner, S. A dynamic discrete network design problem for maintenance planning in traffic networks. *Annals of Operations Research*, **2017**, 253, 757-772

18. Sofronova, E.A.; Belyakov, A.A.; Khamadiyarov, D.B. Optimal Control for Traffic Flows in the Urban Road Networks and Its Solution by Variational Genetic Algorithm. *Procedia Computer Science*, **2019**, 150, 302-308.

19. Celtek, S.A.; Durdu, A.; Alı, M.E. Real-time traffic signal control with swarm optimization methods. *Measurement*, **2020**, 166, 108206.

20. An, H.K.; Abdalla, A.N. Prediction of queuing length at metering roundabout using adaptive neuro fuzzy inference system. *Measurement and Control*, **2019**, 52, 432-440.

21. Azhar, A.M.; Svante, B. Signal Control of Roundabouts. *Procedia-Social and Behavioral Sciences*, **2011**, 16, 729-738.

22. Mosslemi, M. Using Metering Signals at Roundabouts with Unbalanced Flow Patterns to Improve the Traffic Condition: The Case Study of Kannik Area in Stavanger. Master Thesis, Linköping University, Department of Science and Technology, Norrköping, Sweden, 2008.

23. Akçelik, R. Analysis of Roundabout Metering Signals. Paper presented at the 25th AITPM National Conference, Melbourne, Australia, 2006.

24. An, H.K.; Yue, W.L.; Stazic, B. Estimation of Vehicle Queuing Lengths at Metering Roundabouts. *Journal of Traffic and Transportation Engineering (English Edition)*, **2017**, 4, 545-554.

25. Bin, S.; Cui, Z.; Dai, C.; Chen, W. DV-Hop Localization Algorithm with Cuckoo Search. *Sensor Letters*, **2014**,12, 444-447.

26. Zhang, M. Hybrid multi-objective cuckoo search with dynamical local search. *Memetic Computing*, **2017**, 10, 1-10.

27. Cao, Y.; Zhang, H.; Li, W.; Zhou, M.; Zhang, Y.; Chaovalitwongse, W.A. Comprehensive learning particle swarm optimization algorithm with local search for multimodal functions, *IEEE Transactions on Evolutionary Computation*, **2018**, 23, 718-731.

28. Xu, Y.; Qu, R.; Renfa, L. A simulated annealing based genetic local search algorithm for multi-objective multicast routing problems, *Annals of Operations Research*, **2013**, 206, 527-555.

29. Soliman, O.S.; Elgendi, E.A. A hybrid estimation of distribution algorithm with random walk local search for multimode resource-constrained project scheduling problems. *International Journal of Computer Trends and Technology*, **2014**, 8, 57–64.

30. Slavin, C.; Feng, W.; Figliozzi, M.; Koonce, P. Statistical study of the impact of adaptive traffic signal control on traffic and transit performance. *Transportation Research Record*. **2013**, 2356, 117-26.

31. Suksri, C. ANALYSIS AND APPLICATION OF TRAFFIC SIGNAL CONTROL DATA. Ph.D. Thesis, University of South Australia, Department of Transport System Engineering, Adelaide, South Australia, 2012.

32. Dewees, D.N. Estimating the time costs of highway congestion. *Econometrica: Journal of the Econometric Society*, 1979, 1499-1512.

33. Paz, A.; Molano, V.; Gaviria, C. Calibration of corsim models considering all model parameters simultaneously. Proceedings of the 15th International IEEE Conference on Intelligent Transportation Systems, IEEE, 16-22 September 2012, Anchorage, USA.

34. Vasconcelos, L.; Silva, A.B.; Seco, A.; Silva, J. Estimating the parameters of Cowan's M3 headway distribution for roundabout capacity analyses. *The Baltic Journal of Road and Bridge Engineering*. **2012**, 7, 261-8.

35. Feldman, O. The GEH Measure and Quality of the Highway Assignment Models, Association for European Transport and Contributors, London. UK, 2012, 1-18.

 doi:10.20944/preprints202010.0366.v1

36. Vuk, G.; Hansen, C.O. Validating the passenger traffic model for Copenhagen, *Transportation*, **2006**, 33, 371-392.